Global NEST Journal, Vol 25, No 4, pp 23-33

Airborne dust and associated metals: a link between its impact and sink rate within different roadside plants

Rahul M.M.C.* and Saraswathi R.
Department of Civil Engineering, Coimbatore Institute of Technology, Coimbatore, Tamilnadu, India
Received: 17/12/2022, Accepted: 04/01/2023, Available online: 05/01/2023
*to whom all correspondence should be addressed: e-mail: mmcrahul@gmail.com
https://doi.org/10.30955/gnj.004656

GRAPHICAL ABSTRACT

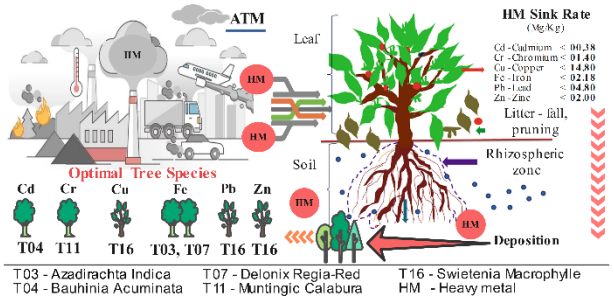

Abstract

Transportation driven by fossil fuels increases air pollution induced by urbanisation. Heavy metals such as Cadmium (Cd), Chromium (Cr), Copper (Cu), Iron (Fe), Lead (Pb), and Zinc (Zn) are life-threatening elements and their concentration is increasing alarmingly in soil in various countries. Air pollution and associated metals contaminate the environment and affect nature's abiotic and biotic components. The significance of tree species originates from their connection to the effects of pollution and the solution approach to their biological cycle. Nineteen distinct tree species dominate the region, with heavy metals sinking in the range of Cd<0.4, Cr<1, Cu<15, Fe<2, Pb<5, and Zn<2 mg/kg or parts per million. According to the findings of this study, tree species can sink heavy metals. The different trees have distinct metals-sink ratios. The competence results showed the order of heavy metal sink as Delonix Regia-red (4) > Delonix Regia-yellow (4) > Syzygium Cumini (3) > Muntingic Calabura (3) of the trees with the highest sink rates and nine species had absorbed lead metal. The nine tree species were unsuitable for heavy metal absorption or deposition. There, Albizia Lebbeck (T02), Biancaca Decapetela (T05), Brucea Javanica (T06), Ficus Elastica (T09), Ficus Religiosa (T10), Pithecellobium Dulce (T13), Tamarind (T17), Terminalia Catappa (T18), and Thespesia Populnea (T19) were very low, less than 10% of other dominant tree species. Syzygium cumini (T16) is a high-yielding tree species that absorb significant quantities of Lead (Pb) and Copper (Cu). These studies confirm that, tree species can capture several heavy metals simultaneously from the polluted environment.

Keywords: Air pollution, heavy metal, remediation, sink rate, transportation, tree species

1. Introduction

Road transportation is the only extensively used mode of transportation that provides direct access to the destination. This is a vital relationship between manufacturers and consumers (MoRTH, 2018). The roadways are India's dominant mode of transportation in terms of share in goods, passenger traffic and its contribution to the national economy. Transportation by roadways has remained a preferred mode of transport primarily because of easy access, the flexibility of operations, door-to-door services, and reliability (MoRTH, 2019).

Air pollution led to a significant increase in vehicular traffic compared to other modes of transport. The global burden of disease study estimated 695,000 premature deaths in 2010 due to continued exposure to outdoor particulate matter and ozone pollution for India (Guttikunda *et al.*, 2014). The Indian government has announced new emission standards called Bharat Stage 6 (BS6), which are in effect from April 2020 (Vats *et al.*, 2022). Due to covid-19 pandemic it has been delayed execution. The rate of urban transportation pollution affects the roadside tree species (Saeedi *et al.*, 2009).

The greenbelt infrastructure in urban areas can be adopted as a passive control system to reduce air pollutant concentrations (Tiwari *et al.*, 2019). A dense multilevel forest has a stable $PM_{2.5}$ mitigation effect and strong ability to improve air quality inside the park under severe pollution (Su *et al.*, 2022). We need to immediately evaluate air pollution strategies to improve the management of green belts (Collazo-Ortega *et al.*, 2017).

In this Study Area, Coimbatore's present population was 2.86 million, a 13.38 percentile increase from 2011 (Census-GOI, 2011). Coimbatore is the 16th-largest city in India. For years, the Avinashi road has been Coimbatore, Tamil Nadu's primary corridor. The research area comprises Coimbatore and its suburbs, Chinnampalayam and Nilambur, which are 247 km^2, 17 km^2, and 6 km^2, respectively, as shown in Figure 1. Avinashi road starts

from Grey Town's Uppilipalayam flyover and continues via Peelamedu, Chinniampalayam, and Neelambur, as shown in Annexure -1A. This road links the 16-kilometer east-west portion with a northeast tangent. It has fifteen vital traffic junctions with a location description, as shown in Table 1.

This study reveals a link between the deposition of suspended air pollutants from fossil-fuel-based transportation and impacts on roadside-growing tree species. This study focuses on particulate matters and other pollutants that influence the region's heavy metal deposition. Tree species absorb pollutants and let them sink into their tree components and soil through photosynthesis and leachate. As a result, it has detected the significant heavy metal sink rates of dominant tree species in urban environments, which are necessary to overcome the effects of air pollution.

Table 1. Sampling locations based on the traffic junction

Traffic Junction's	Latitude	Longitude	Sample Locations	Description(Radius ≤ 500 meters)
S01	11.0027	76.9684	C1.	Commercial and traffic area.
S02	11.0038	76.9724	T-AR007, 008G.	Residential and traffic area.
S03	11.0052	76.9747	T-AL029, 31, 32, 33, 34, T-AR009, C2, C3.	Residential and light traffic area.
S04	11.0129	76.9860	T-AR015, 16, T-AL042, 54, 59, 70, 72, C4.	Residential and heavy traffic area.
S05	11.0200	76.9921	C5, T-AL083, 84, 89, C6	Residential, Educational Institutions and Heavy Traffic Areas.
S06	11.0232	77.0016	T-AR070,72, 84, 94.	Educational Institutions and Heavy Traffic Area.
S07	11.0250	77.0103	T-AR104, 105, 119, C7.	Residential Area Closure to Shopping complex (Mall).
S08	11.0258	77.0176	T-AL136,140, T-AR128, 129, 130, C8, C9	Educational Institutions and Heavy Traffic Area.
S09	11.0293	77.0263	T-AR140, 147, 148, 149, 158, 162, T-AL162, 173, 174. C10 to C16.	Heavy Traffic Area.
S10	11.0380	77.0374	T-AR189, 201, T-AL223, C18 to C22.	Residential, Industrial and Airport Areas.
S11	11.0463	77.0520	T-AR214, 223, C23	Residential Area Closure to Hospital, Restaurants
S12	11.0513	77.0598	T-AR259.	Residential and traffic areas.
S13	11.0548	77.0646	C24, C25.	Residential and traffic areas.
S14	11.0611	77.0862	T-AL306, 309, 318, 319, T-AR337, 328, 340.	Residential and Light traffic areas.
S15	11.0647	77.0934	T-AR344, 345, 345G.	Traffic area closure to NH 544.

**AR-Adjust Right Side, AL- Adjust Left Side, C-Cross Section Roadsides, G-Grid Pool.*

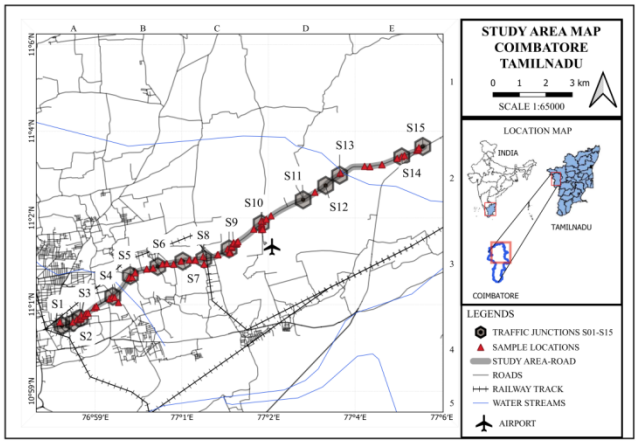

Figure 1. Study area map of sample locations and Traffic intersections

2. Materials and methods

2.1. Sample collection and preparation

Transportation emits significant pollutants to precipitate on the tree's leaves and soil. The significant pollutants accumulated in the tree leaf sample (from bottom to top) and a random soil sample location (1 m*1 m radial silhouette), as shown in Annexure-1A. The samples were dried at 60°C for overnight in a hot air oven (Manufacture: Genuine Equipment, India). The leaf samples were crushed into the powder and sieved with a 150-micron filter (ASTM). The samples are stored and kept in moisture-free containers.

2.1.1. Plant sample preparation

A 1000 mg leave sample was mixed with a10 mL of conc. nitric acid. Then 5 mL of acid-mixture ratio of 1:2:5 (H_2SO_4:$HClO_4$:HNO_3) was added and digested/heated till white perchloric acid (Brand: Millipore, AR Grade 99%) vapours after cooling the sample to 35 mL of distilled water, heated for two hours at 100±5ºC in a mini micro-digestor. The filtered sample was diluted with 50 mL of aspiration with a dilution factor.

2.1.2. Soil sample preparation

Add 2.5ml Nitric acid (HNO_3) and 7.5 mL Hydrochloric acid (HCl) to a 1000 mg soil sample and oven at 120±5ºC for 24 hours. The samples were heated on a hot plate for 2 hours until smoke formed. The solution dilutes the sample volume to 50 mL of distilled water for aspiration (Quartz Double Distillation Unit, Labsil, India).

2.2. Testing apparatus

Heavy metal analytes were determined using FAAS (Atomic Absorption Spectroscopy, Model: TL-3800AA, Manufacturer of Top Lab, India) with Hollow cathode

lamps. The Optimal wavelengths are 228.8, 357.9, 324.8, 248.1, 217, and 213.9. All components have a 2 L/min acetylene flow rate, except Cr. 6 L/min and 0.2 Nm wide. Lean, blue. A slotted tube atom trap (STAT) has boosted the FAAS sensitivity of Cd, Cr, Cu, Fe, Pb, and Zn.

2.2.1. Chemical reagents

The heavy metal elements of Cd, Cr, Cu, Fe, Pb, and Zn are 1000 ppm stock solutions made using the corresponding technique. To prepare a stock solution for Cd, dilute 1 g of cadmium metal in 1 litre (L) of distilled water with 1% HCl. Dissolve 3.735 g potassium chromate (K_2CrO_4) in 1L distilled water to create a Cr stock solution. Dissolve 1 g of copper metal in (1+1) HNO_3 and dilute 1L of distilled water with 1% (v/v) HNO_3. Dissolve 1 g of iron wire in 50 ml of (1+1) HNO_3 to make a Fe stock solution. Dilute with distilled water to 1L. 1.598 g $Pb(NO_3)_2$ was dissolved in 1% (v/v) HNO_3 to form a stock solution (Pb). 1 g zinc metal in (1+1) HCl with 1% (v/v) HCl in 1L distilled water.

2.3. Methodology

Transportation powered by fossil fuels exacerbates air pollution and metal contamination in urban and suburban areas. Traffic intersections and heavily polluted areas had selected as sample locations. The assessment of transportation survey uses the emission factor parameters such as vehicle type, fuel type, model, speed, and emission factors, which aid in determining the traffic pollution rate in specific locations. These contaminants spread across the air medium because of meteorological conditions. Vehicle emissions significantly impact roadside-growing tree species and the related metals that arise in tree species due to air-borne emissions.(Bisht *et al.*, 2022) An attempt to predict the sink rate plant species and their rightful place in the urban environment process flow chart, as shown in Figure 2.

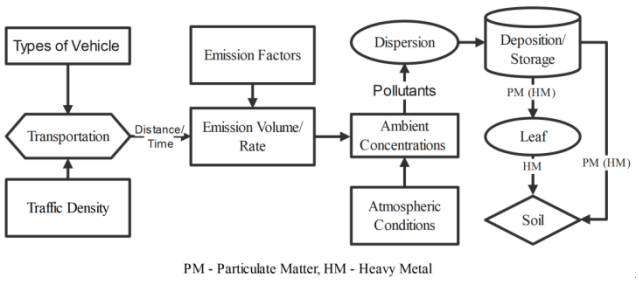

Figure 2. Heavy Metal's Capturing from Roadside Emissions

3. Result and discussions

Empirical methods and fossil-fuel-powered transportation were used to compute air pollution emissions. Then, air quality and traffic were examined. The correlated transportation-related heavy metals mobilise roadside trees. The maximum heavy metal sink rate of tree species and regional impacts were determined.

3.1. Transportation

The road transport sector in India has grown exponentially in terms of connectivity since its independence. The number of registered vehicles on the road and the volume of passengers and cargo handled by road transport has increased drastically (McNabola *et al.*, 2009). Coimbatore has 20,54,491 registered vehicles, 16,30,079 (Two-wheelers-2w), 11,726 (Three-wheelers-3w), 2,65,902 (LMV- Light Multi-role Vehicles), and 13,471 (Heavy motor vehicles-HMV). Commercial vehicles include 12,134 (3w), 16,784 (LMV) and 1,04,495 HMV. (Road and Transport, 2020).

3.1.1. Passenger car unit

Passenger Car Unit (PCU) measures the relative interaction between a vehicle and a traffic stream concerning a standard passenger car under a specified roadway and traffic conditions.(CSIR-CRRI, 2017).

The simultaneous equations method is also a headway-based approach for estimating PCU. A simultaneous equation for similar traffic conditions has been determined as shown in Table 2. There are several iterative techniques for solving in the literature. It is more accurate than the multiple linear regression method (Dhamaniya and Chandra, 2016). Its iteration process makes the calculations too lengthy and tedious.

If h_1 is the average headway for all-car situations and h_{mix} is that for a mixed traffic stream, the volume of all car traffic (Q_1) and mixed traffic (Q_m), P_i = proportion of vehicle category 'i', PCU_i = PCU of vehicle category 'i', n = number of vehicle categories is calculated as given below. (Sharma and Biswas, 2021)

The average headway of a mixed traffic stream is further defined as,

$$h_{mix} = h_1 \sum_{i=1}^{n} (P_i \times PCU_i) \quad (1)$$

Hence,

$$\frac{h_{mix}}{h_1} = \frac{Q_1}{Q_m} \sum_{i=1}^{n} (P_i \times PCU_i) \quad (2)$$

$$Q_1 = Q_m \sum_{i=1}^{n} (P_i \times PCU_i) \quad (3)$$

3.1.2. Traffic data (ADT-2021)

The high traffic congestion locations at signal sites have been conducted to collect data on traffic flow(Acosta *et al.*, 2014; Huang *et al.*, 2022). This data was considered for the traffic research and evaluated for both directions of moving vehicles, turning, and merging vehicles at the junction of prominent road signal locations. The research region's high traffic density signal position is S4 to S12, as shown in Table 2. Due to incomplete combustion, unburned hydrocarbons (HC) are released inraffic-conjugated environments (Hao *et al.*, 2022). Fossil fuels consumed in automotive engines emit CO, NOx, PMs, and HC (Amato *et al.*, 2014). It contributes to air pollution.

Table 2 shows the vehicle types, volumes, and sampling locations for ADT. Here, ADT observed data for one month (PH of GMT+5:30 are 08:00 to 10:00,12:00 to 13.00,16:00 to 21:00 & NPH-Non-peak hours) and calculated PCU concerning the standard coefficients of 2W, 3W, LMV, and HMV were 0.5, 1.0, and 3.0, respectively. The coefficients

are multiplied by their vehicle types and the sum of the total values.

3.2. AAQ data

The ambient air quality (AAQ) statistics were carried out using one-year data from the central pollution control board (CPCB) for study locations. The air pollutants were present in the average atmospheric bar pressure of 961.67 [mbar] and the global horizontal irradiance of 193.78 GHI [W/m^2] in the metrological conditions over the period (Solcast, 2021). The parameters are particulate matter's, gaseous pollutants, and wind data(CCR, 2021) from the CPCB, as shown in Figure 3 and the Summary Statistics for Annual Ambient Air Quality Data (2021), as shown in Annexure-2A.

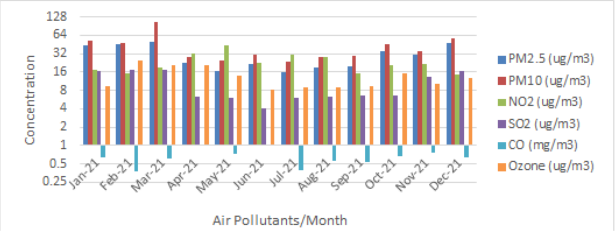

Figure 3. Air pollutants fluctuating in the locations

3.2.1. Wind data

The significant wind concentration in the blowing direction to the East-North-East (ENE) to above 13 percentiles, and the subsequent blowing-to-wind direction is Northeast to 7 percentiles. The wind diagram builds by the 8735 hours for one year on the sample location. In this study area, the average wind is 1.93 m/s, and the calm wind direction is 3.63 % through the year (2021), as shown in Annexure-3A.

3.3. Identification of tree species

The Tamilnadu Forest department, India found several categories of tree species in the Coimbatore district. One of the essential groups is the pollution control tree species. The leaf shape identifies the tree species (Truncate, Lanceolate, Elliptical, Oval, Linear) and arrangement (simple & compound) of leaf edges or margins (Entire leaf, lobed leaf, toothed leaf, parted leaf). Leaf Veins and Venation Patterns (Pinnate, Palmate), structure, shape (Columnar, Open-head Irregular, Weeping, Pyramidal, Globe-shaped, Fastigiate, Vase-shaped and Horizontal spreading). Bloom growth and petal fall (Flower).

In the study area, green cover is nearly 740 trees on both roadsides for a 15 km stretch length, and 19 different tree species were considered. The predominant tree has present in the location is Pongamia Pinnata (L)> Ficus Religiosa> Delonix Regia-Red, Royal Poinciana> Albizia Julibrissin> Azadirachta Indica> Thespesia Populnea> Delonix Regia-Yellow, Royal Poinciana> Tamarind Tree> Terminalia Catappa> Bauhinia Acuminata Leaves> Muntingic Calabura> Swietenia Macrophylle> Syzygium Cumini>Pisonia Grandis>Pithecellobium Dulce> Albizia Lebbeck>Brucea Javanica>Ficus Elastica.

3.4. Heavy metal impact

Heavy metals are well-known environmental pollutants due to their toxicity, persistence in the environment, and bio-accumulative nature (Anerao *et al.*, 2022). Motor vehicle emissions are a major source of airborne contaminants including arsenic, cadmium, cobalt, nickel, lead, antimony, vanadium, zinc, platinum, palladium, and rhodium (Ayres, 1997). The tree species capable of capturing several heavy metals simultaneously, and they are called as Valuable Phytoremediation Process (Pouresmaieli *et al.*, 2022).

Table 2. Traffic Study Data (ADT-2021)

Location Code	PH				NPH				PCU		ADT
	2W	3W	LMV	HMV	2W	3W	LMV	HMV	PH	NPH	
S1	8945	514	7868	24492	3448	81	1890	233	17137	4353	24492
S2	9231	526	7884	24337	3779	80	1538	220	16000	4126	24337
S3	6951	314	6517	19187	2085	94	1955	293	13082	3925	19187
S4	15826	335	6440	30577	3479	198	2972	407	17280	6031	30577
S5	22511	527	12244	47580	4817	310	5230	623	27716	9661	47580
S6	25718	563	9494	48047	4990	302	4631	1165	26188	10773	48047
S7	15936	1096	14781	44147	4781	329	4434	644	29736	8921	44147
S8	24910	1656	26227	73476	7957	547	7380	1072	50691	14847	73476
S9	25271	1628	27435	74879	7616	506	8018	1139	50683	15498	74879
S10	33830	2631	25234	85019	10149	789	7570	1111	54579	16374	85019
S11	18225	1412	13854	46331	5520	430	4125	616	30118	8950	46331
S12	11784	1068	10795	32604	3848	298	2925	454	21518	6358	32604
S13	6879	624	6301	19032	2064	187	1890	251	12561	3768	19032
S14	9958	221	3730	18875	2988	66	1119	183	10651	3195	18875
S15	12326	289	6704	26052	3698	87	2011	216	15176	4553	26052

**PH-Peak hours, NPH-Non-peak hours, Two-wheelers (2W), Three-wheelers (3W), Light Multi-role Vehicles (LMV), and Heavy motor vehicles (HMV), Passenger car unit (PCU), and Average daily traffic (ADT).*

3.4.1. Calibration standards

A calibration curve is used in analytical chemistry to determine an unknown concentration in a solution. The FAAS calibrates the known stock concentrations (1–10 ppm) and the element's corresponding lamp wavelength.

The unknown solution's absorbance and a calibration curve were measured between the concentration and absorbance readings. Regression equations for the calibration of heavy metals are as below,

$$Y = 0.0724x - 0.0024 = 0.9939 = R^2 \text{ for Cadmium} \quad (4)$$

$$Y = 0.0145x + 0.0053 = 0.9974 = R^2 \text{ for Chromium} \quad (5)$$

$$Y = 0.1044x + 0.0440 = 0.9926 = R^2 \text{ for Copper} \quad (6)$$

$$Y = 0.1987x + 0.1230 = 0.9910 = R^2 \text{ for Iron} \quad (7)$$

$$Y = 70.3490x - 3.2869 = 0.9966 = R^2 \text{ for Lead} \quad (8)$$

$$Y = 0.1044x + 0.0440 = 0.9926 = R^2 \text{ for Copper} \quad (9)$$

3.4.2. Leaf analysis

Te species remove air pollution by the interception of particulate matter on plant surfaces and absorbing pollutants through the leaves (Nowak *et al.*, 2014). The particulate matter is in the combined forms of associated metals called heavy metals (Chen *et al.*, 2021). These are captured or trapped on the leaf surface. The analysis result indicates that the leaf captures the heavy metals at different levels concerning the tree species.

The Pearson Coefficients of Leaf Samples in the heavy metal cbination of Cd: Zn is 0.12 to 0.24, exhibiting a negative linear connection to the other heavy metals. Then, the leaf samples combination of the Cu: Cr is 0.08 and Fe: Cu is 0.01, resulting in a negative linear correlation, wreas other metal combinations show a positive interaction of the Cu: Cr is 0.02 to 1, Fe: Cu is 0.3 to 1, and Zn: Pb is 0.6.

Pollutants are predominantly present in the upper layer of theeaf, and the rate of heavy metal absorption/sink from air-borne pollutants varies according to tree species. In Figure 4, exposes that the Cadmium of S10, S13, S14, and S15 is below 0.12 ppm. Furthermore, S6, S7, S11, and S12 are greater than 0.5 ppm. Copper level in S9 and S10 ranges from 1.6-2.2 ppm, whereas S14 exceeds 2.2 ppm. It also has an impact on the S13 and S15 sites. The iron impact on S10, S11, and S12 ranges from 0.8 to 1.6 ppm, whereas S13 exceeds 3.2 ppm and influences the S14 position. The lead impact is 0.9-1.4 ppm on S7, S13, S14, and S15, and 1.90 ppm between S8 and S9.

The location of S3, S4, S5, and S6 had a lower pollution level of 0.5 ppm compared to other places. S3, S4, S5, and S6 are 0.4-0.8 ppm, S13 is 0.8-1.2 ppm, and S8, S9, S10, and S13 are more than 1.6 ppm. The accumulation of air pollution sediment on roadside tree leaves demonstrates how critical it is for transportation and incineration activities in locations without clean air from industries, as shown in Figure 4.

3.4.3. Soil analysis

The soil sample's respective heavy metals are interpolated range to the Cd of 0.03<0.1, Cr of 0.9<2.5, Cu of 0.3<0.9, Fe of 4.8<6.6, Pb 0.5< 1.3 and Zn 0.4<3.3 with confidence level (95%) from the result of 14 sampling location. These outcomes indicate to the standards that these heavy metals, Zn< Pb<Cr, are contaminated on their location from a soil sample taken. These location tree species highly sequester the heavy metal elements in the soil.

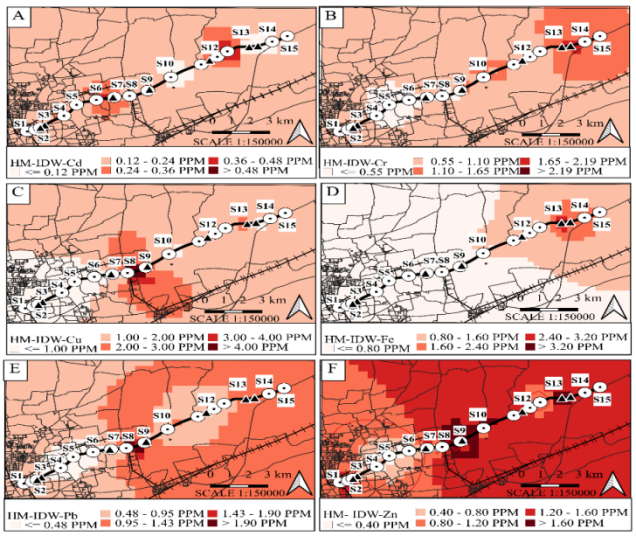

Figure 4. Impact on the leaf

The heavy metal of the Cd: Zn is 0.13 to 0.20 combination and Cu is 0.02 have a negative linear correlation in the other Heavy metals. Then, the Fe: Cr is 0.43, Fe: Cu is 0.47 and Fe: Pb is 0.27 combination results in negative linear correlations, and other combinations of Heavy metals indicate the positive correlation range is 0.1 to 0.5 for the soil samples.

The sample results in Figure 5 illustrate the reflection in traffic intersections and the contamination levels of various heavy metals in soil areas—the Cadmium levels in S6, S7, S8, S11, and S12 range from 0.12-0.16 ppm. Chromium levels in S13, S14, and S15 vary between 2.0 and 3.0 ppm. Copper values in S6, S7, S8, S9, S10, S11, S12 range from 0.4-0.6 ppm and S13, S14, and S15 are and 0.6-0.8 ppm. S12, S13, S14, and S15 have iron levels less than 6.2 ppm, whereas S1, S2, S3, and S4 have iron levels between 6.35 and 6.4 ppm. Furthermore, S5, S6, S7, S8, S9, and S10 have more than 6.4 ppm. Lead values in S1, S2, S3, S4, S5, and S6 vary from 0.7 to 0.9 ppm, while 1 ppm in S11, S12, S13, S14, and S15. Zinc concentrations in S13, S14, and S15 range from 1.5–2 ppm, whereas S11 and S12 exceed 2 ppm.

3.5. HM deposition

In response to deposition in diverse tree species, the rate at which heavy metals sink in the leaf and soil has changed according to age, absorption rate, and traffic intensity of locations. The result depicts the cumulative impact of several tree species on the heavy metal sink, as shown in Figure 6. The maximum concentration of heavy metals in an area can help to determine individual tree species' concentration and sinking rate. Annexure-1A and Table 3 were used to predict which tree species can sink heavy metals by determining their locations and absorption rates.

Table 3. HM in Soil and leaves -Cluster of tree species

Sample locations	Heavy Metals Concentration (ppm)											
	Cd		Cr		Cu		Fe		Pb		Zn	
	^	˅	^	˅	^	˅	^	˅	^	˅	^	˅
S1	BDL	0.20	BDL	0.50	BDL	0.28	BDL	0.19	BDL	0.13	BDL	0.24
S2	0.29	0.55	3.52	7.04	0.92	1.69	BDL	1.24	1.34	3.99	6.29	
S3	0.18	0.34	0.67	2.67	0.41	1.72	1.49	6.41	0.54	1.34	0.85	2.56
S4	0.22	0.41	0.61	2.68	0.44	1.95	0.22	0.38	0.52	0.92	0.69	2.60
S5	0.19	0.26	0.14	0.15	0.12	0.14	0.22	0.27	0.23	0.31	0.18	0.21
S6	0.29	0.44	0.28	0.45	0.25	0.32	0.17	0.30	0.10	0.28	0.24	0.29
S7	0.29	0.41	1.07	1.71	0.38	0.71	1.97	6.49	0.79	1.19	1.41	2.66
S8	0.20	0.47	0.17	0.34	7.52	44.53	0.40	1.55	2.67	14.54	1.95	6.02
S9	0.20	0.44	1.50	5.07	0.62	2.13	2.27	6.58	0.82	1.29	1.44	3.22
S10	0.03	0.07	1.01	4.19	1.07	7.20	1.15	4.96	0.62	1.19	1.16	2.86
S11	0.06	0.09	0.83	1.66	0.46	0.52	3.06	6.12	1.09	1.19	2.19	2.53
S12	BDL	0.09	BDL	1.65	BDL	0.40	BDL	6.11	BDL	1.00	BDL	2.54
S13	0.16	0.62	1.74	2.52	0.90	3.00	4.03	6.59	1.06	1.50	1.46	3.27
S14	0.05	0.06	2.15	2.53	0.73	0.94	6.46	6.53	1.00	1.05	1.99	3.26
S15	BDL	0.09	BDL	1.99	BDL	0.83	BDL	BDL	1.44	BDL		1.64

**BDL-Below detectable limit, ^ Indicates minimum value, and ˅ Indicates Maximum Value.*

Table 4. Average sink rate of HM

T	Tree Species	Cd	Cr	Cu	Fe	Pb	Zn	CE	PSE	C %	Sink Grade
T01	Albizia Julibrissin	BDL	0.01	0.90	0.19	0.30	0.42	Cr, Cu, Fe, Pb, Zn	Pb, Zn	33	08
T02	Albizia Lebbeck	0.01	0.11	0.06	0.17	0.07	0.10	Cd, Cr, Cu, Fe, Pb, Zn	-	-	14
T03	Azadirachta Indica	0.01	0.34	0.68	1.28	0.29	0.45	Cd, Cr, Cu, Fe, Pb, Zn	Cr, Fe, Pb, Zn	50	05
T04	Bauhinia Acuminata Leaves	0.38	0.32	0.29	0.32	0.18	0.21	Cd, Cr, Cu, Fe, Pb, Zn	Cd, Cr	33	07
T05	Biancaca Decapetela	0.02	0.06	0.01	0.07	0.07	0.11	Cd, Cr, Cu, Fe, Pb, Zn	-	-	15
T06	Brucea Javanica	BDL	BDL	BDL	0.17	0.12	0.30	Fe, Pb, Zn	Pb, Zn	33	12
T07	Delonix Regia-Red	0.02	0.72	0.30	1.90	0.33	0.68	Cd, Cr, Cu, Fe, Pb, Zn	Cr, Fe, Pb, Zn	67	01
T08	Delonix Regia-Yellow	0.02	0.60	0.19	1.20	0.30	0.69	Cd, Cr, Cu, Fe, Pb, Zn	Cr, Fe, Pb, Zn	67	02
T09	Ficus Elastica	0.01	0.02	0.01	0.01	BDL	0.01	Cd, Cr, Cu, Fe, Zn	-	-	16
T10	Ficus Religiosa	0.01	0.01	0.01	0.01	0.01	0.01	Cd, Cr, Cu, Fe, Pb, Zn	-	-	17
T11	Muntingic Calabura	0.02	1.40	BDL	0.67	0.28	0.57	Cd, Cr, Fe, Pb, Zn	Cr, Fe, Pb, Zn	50	04
T12	Pisonia Grandis	0.08	0.07	0.07	0.06	0.12	0.01	Cd, Cr, Cu, Fe, Pb, Zn	Cd, Pb	33	10
T13	Pithecellobium Dulce	0.01	0.03	0.02	0.01	0.01	0.01	Cd, Cr, Cu, Fe, Pb, Zn	-	-	18
T14	Pongamia Pinnata (L)	0.03	0.39	0.15	0.32	0.15	0.30	Cd, Cr, Cu, Fe, Pb, Zn	Cr, Pb	33	09
T15	Swietenia Macrophylle	0.05	0.89	0.21	0.03	0.46	0.38	Cd, Cr, Cu, Fe, Pb, Zn	Cd, Cr, Pb	50	06
T16	Syzygium Cumini	BDL	BDL	14.84	BDL	4.83	2.00	Cu, Pb, Zn	Cu, Pb, Zn	50	03
T17	Tamarind Tree	0.01	0.11	0.06	0.17	0.07	0.10	Cd, Cr, Cu, Fe, Pb, Zn	-	-	19
T18	Terminalia Catappa	0.08	0.06	0.07	0.02	0.01	0.07	Cd, Cr, Cu, Fe, Pb, Zn	Cd	17	13
T19	Thespesia Populnea	0.06	BDL	BDL	0.05	0.06	0.46	Cd, Fe, Pb, Zn	Cd, Zn	33	11

**BDL-Below detectable limit, T- Tree species, CE-Capturing elements, PSE-Predominate sink elements, and C%-Competence percentile.*

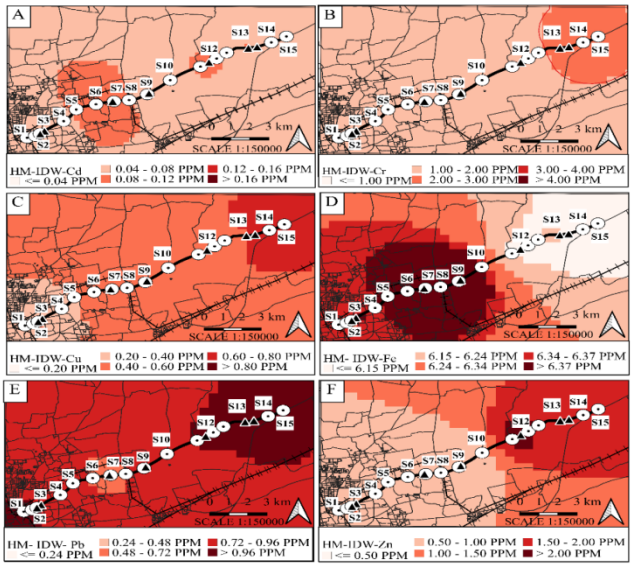

Figure 5. Soil Impact

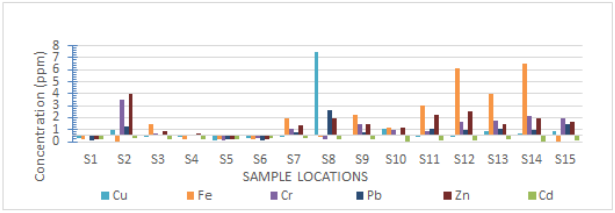

Figure 6. Heavy Metal Depositions

The different tree species can sink heavy metals as follows for a maximum range of Cd < 0.4, Cr < 1.4, Cu < 14.8, Fe < 2.2, Pb < 4.8 and Zn < 2 ppm in the region of individual tree species. Except for the high-yield tree species of Syzygium Cumini (T16), it absorbs a large amount of Lead and copper sink, and nine tree species were unsuitable for heavy metal deposition or absorption. There, the viability percentages of Albizia Lebbeck (T02), Biancaca Decapetela (T05), Brucea Javanica (T06), Ficus Elastica (T09), Ficus Religiosa (T10), Pithecellobium Dulce (T13), Tamarind (T17), Terminalia Catappa (T18), and Thespesia Populnea (T19) were very low, less than 10% of other dominant tree species.

The Analytic results in Table 4 Shows, which tree species can sink heavy metal on itself. These tree species have a high sink rate of different heavy metals are Delonix Regia-Red, (T07- Cr, Fe, Pb, Zn) > Delonix Regia-yellow (T08 - Cr, Fe, Pb, Zn) > Syzygium Cumini (T16- Cu, Pb, Zn)> Muntingic Calabura (T11- Cr, Fe, Pb, Zn) >Azadirachta Indica (T03- Cr, Fe, Pb, Zn) > Swietenia Macrophylle (T15- Cd, Cr, Pb) > Pisonia Grandis (T12- Cd, Pb) > Pongamia Pinnata (T14- Cd, Pb) >Bauhinia Acuminata Leaves (T01- Cd, Cr)> Albizia Julibrissin (T01- Pb, Zn).

The best sink respect to their metals is Bauhinia Acuminata Leaves (T04) for Cd, Muntingic Calabura (T11) for Cr, Syzygium Cumini (T16) for Cu, Pb, and Zn, Azadirachta Indica (T03) and Delonix Regia-Red (T07) for Fe.

3.6. Communal Index

The Communal index (CI) finds the different heavy metal's complex effects on the level of contamination of their tree species for traffic-polluted locations and the overall impact on the traffic Junction locations. The individual tree species highly affected by their location for T-AR149>162>295>147S>148S>104S>119>94, T-AL318S> 31>31S>309S> 319S>319>29>, C25>C11>C1. The distance from the roadside or cross-sectional roadside indicates that pollution decreases due to transportation density. It helps to determine the index, as shown in Figure 7.

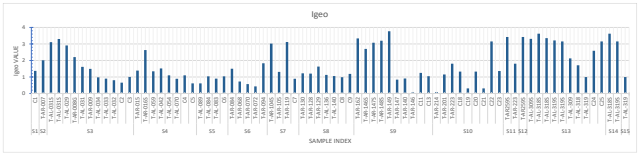

Figure 7. Communal Index at Individual Locations

3.6.1. Communal Contamination level

The traffic junction is heavily (Strongly) contaminated for index class 4 to the locations S2, S8, S9, S11, S12, S13, S14, and S15. Under the index class of 3, S3, S4, S7, and S10 are moderate to heavily (Strongly) contaminated. S1 and S6 in class 2 are moderately contaminated, and S5 under the index class of 1 for uncontaminated locations to moderately contaminated, as shown in Table 5 and Figure 8. The overall regression in heavy metal combination effect is Cd to other metals and Fe: Cu combinations are negative liner coefficients that restrict beyond forwarding correlation.

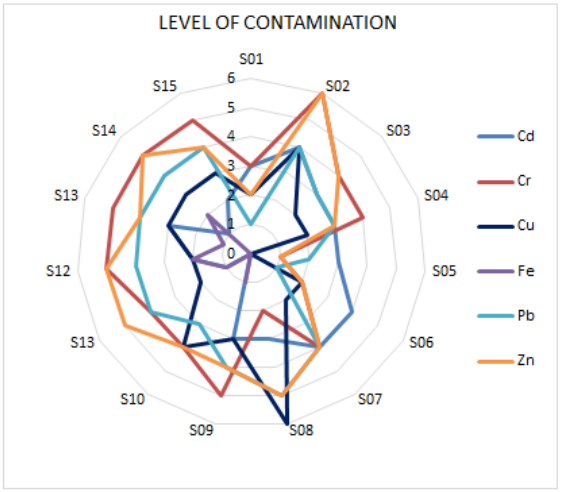

Figure 8. Overall Heavy Metals Intensity Rate at Traffic Junctions

3.6.2. Communal Numerical Forecast

Numerical prediction is the practice of mathematical values of transportation emission factors and heavy metal coefficients present in tree species to predict the impact of air pollution based on actual communal heavy metals impact conditions. The coefficients to the individual parameter of heavy metal have combined the effect of the sample locations. Hence, Predicated impact (P*i*) formula,

$$P_i = \begin{bmatrix} 1.7165(Cd) + (-0.1058(Cr)) + (-0.2002(Cu)) \\ +0.3101(Fe) + 0.6214(Pb) + 0.1066(Zn) + 0.6102 \end{bmatrix} \quad (10)$$

The equation helps find the heavy metal mixed composition to the collective impact from the transportation roadside area. The equation for the overall error is 1.2709 with a 95% confidence limit, as shown in Annexure-4A. The sum of the square is less than 0.45, the degree of freedom is 76, its theoretical value is less than the experimental value, and the square of R is 0.62, which indicates the non-linear equation from 76 observations. It indicates that the model is significate in predicting the equation from the ANOVA.

Table 5. Interpolation of heavy metal overall Impact at Traffic Junctions

L	Igeo Index Values						Avg. Index	Index class	Level of Contaminations
	Cd	Cr	Cu	Fe	Pb	Zn			
S1	3	3	2	0	1	2	1.6	2	Moderately contaminated
S2	4	6	4	0	4	6	4	4	Heavily (strongly) contaminated
S3	3	4	2	0	3	4	2.6	3	Moderately to heavily (strongly) contaminated
S4	3	4	2	0	3	3	2.4	3	Moderately to heavily (strongly) contaminated
S5	3	1	0	0	2	1	0.8	1	Uncontaminated to moderately contaminated
S6	4	2	2	0	1	2	1.4	2	Moderately contaminated
S7	4	4	2	0	4	4	2.8	3	Moderately to heavily (strongly) contaminated
S8	3	2	6	0	5	5	3.6	4	Heavily (strongly) contaminated
S9	3	5	3	1	4	4	3.4	4	Heavily (strongly) contaminated
S10	0	4	4	0	3	4	3	3	Moderately to heavily (strongly) contaminated
S11	1	4	2	1	4	5	3.2	4	Heavily (strongly) contaminated
S12	2	5	2	2	4	5	3.6	4	Heavily (strongly) contaminated
S13	3	5	3	1	4	4	3.4	4	Heavily (strongly) contaminated
S14	1	5	3	2	4	5	3.8	4	Heavily (strongly) contaminated
S15	2	5	3	0	4	4	3.2	4	Heavily (strongly) contaminated

4. Conclusions

Heavy metal elements are causing a sinking level difference in roadside tree species. Tree species do not absorb all the elements from the air into the soil. The exposed area of the leaves adheres to the heavy metal was deposited by transpiration and photosynthesis, depending on the tree type. The variable conditions can cause some heavy metals to settle straight into the soil.

The study illustrates how pollution has affected roadside tree species, pollution rate, emission factors, air contaminants, and atmospheric conditions over geological periods. These discoveries led to the development of therapeutic solutions derived from several tree species. the high-yield tree species of Syzygium Cumini (T16), it absorbs a large amount of Lead and copper sink, and nine tree species were unsuitable for heavy metal deposition or absorption. There, the viability percentages of Albizia Lebbeck (T02), Biancaca Decapetela (T05), Brucea Javanica (T06), Ficus Elastica (T09), Ficus Religiosa (T10), Pithecellobium Dulce (T13), Tamarind (T17), Terminalia Catappa (T18), and Thespesia Populnea (T19) were very low, less than 10% of other dominant tree species.

These analytic results have contributed to establishing green belts for suitable tree species in urban transportation and dense traffic areas, reducing the heavy metal pollution they cause. During this research, the young (<15 years) tree species are more efficient in absorbing the heavy metal to sink on themselves. This study helps to place the suitable tree species necessary in their polluted or contaminated environments. The step-by-step transformation of a tree by continuous real-time monitoring over the geologic period is obligatory.

Author Contribution

Corresponding Author – Roles of Conceptualization, Formal analysis, Investigation, Writing - Original Draft, Visualization.

Co-author - Roles of Methodology, Validation, Resources, Writing - Review & Editing, Supervision

Conflict of Interest

The authors state that they have no known financial or personal relationships that could have influenced their research work.

Acknowledgements

This heavy metal testing was conducted using Atomic Absorption Spectroscopy, Model: TL-3800AA, Manufacturer of Top Lab, India, as part of the TEQIP-III Equipment at the Environmental Engineering Laboratory, Coimbatore Institute of Technology, Tamilnadu, India.

Annexure-1A

Tree Species & Soil No. Information

Locations	Locality-Signal	Lat.	Long.	Leaf Species No.	Soil No.
S1	Uppilipalayam	11.0027	76.9684	C1	-
S2	VOC Park	11.0038	76.9724	T-AR007, T-AR008G	-
S3	Anna Salai	11.0052	76.9747	T-AL029, 31, 32, 33, 34, T-AR009, C2, C3	T-AL031S
S4	Lakshmi mills	11.0129	76.9860	T-AR015, 16, T-AL042, 54, 59, 70, C4, C5	T-AR016S
S5	Nava India	11.0200	76.9921	T-AL083, 84, 89, C6	-
S6	PSG Tech	11.0232	77.0016	T-AR068, 70,72, 84, 94.	-
S7	Fun mall	11.0250	77.0103	T-AR104, 105, 119, C7	T-AR104S
S8	Hope college	11.0258	77.0176	T-AL136, 140, T-AR128, 129, 130, C8, C9	-
S9	CODISSIA	11.0293	77.0263	T-AR140, 146, 147, 149, T-AL162, C11, C13	T-AR146S, 147S,148S
S10	SITRA	11.0380	77.0374	T-AR189,201,214, T-AL223, C18, 19, 20, 21, 22, 23	-
S11	Thottipalayam Pirivu	11.0463	77.0520	T-AR223	-
S12	R.G. Pudur	11.0513	77.0598	T-AR259	T-AR259S
S13	Chinniampalayam	11.0548	77.0646	T-AL309	T-AL309S
S14	Neelambur	11.0611	77.0862	T-AL318	T-AL318S
S15	PSG Foundry	11.0647	77.0934	T-AL319	T-AL319S

Annexure-2A

Summary Statistics for Annual Ambient Air Quality Data (2021)

Parameters	$PM_{2.5}$	PM_{10}	NO_2	SO_2	CO	Ozone	RH	WS	WD
Units	ug/m^3	ug/m^3	ug/m^3	ug/m^3	mg/m^3	ug/m^3	%	m/s	Degree
Mean	30.64	42.5	23.22	10.23	0.66	13.59	72.87	8.58	153.34
Standard Error	3.76	6.62	2.53	1.56	0.06	1.62	3.86	0.97	17.6
Median	26.67	32.88	21.32	6.6	0.63	11.43	77.7	8.14	153.59
Standard Deviation	13.01	22.94	8.75	5.39	0.2	5.62	13.39	3.37	60.98
Sample Variance	169.33	526.05	76.54	29.08	0.04	31.55	179.2	11.35	3718.59
Range	32.97	81.96	29.27	13.33	0.65	16.3	38.85	9.28	168.34
Minimum	16.21	23.74	14.38	4.07	0.38	8.21	45.4	4.76	74.67
Maximum	49.18	105.7	43.66	17.4	1.02	24.5	84.25	14.04	243.01
Sum	367.74	510	278.67	122.77	7.95	163.03	874.39	103	1840.11
Confidence Level (95%)	8.27	14.57	5.56	3.43	0.13	3.57	8.51	2.14	38.74

Annexure-3A

Wind Rose Diagram:

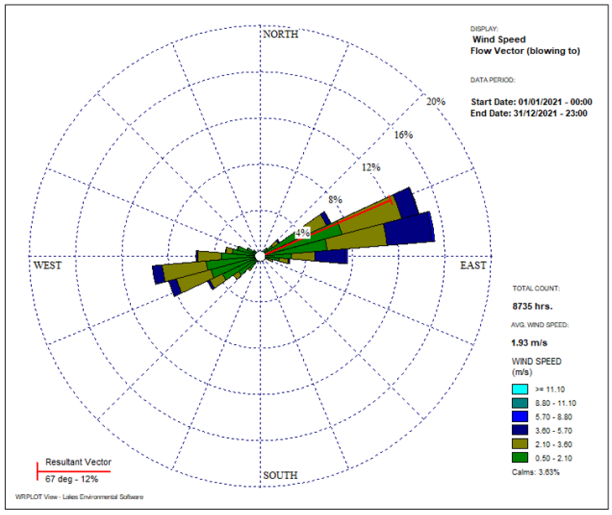

Wind Rose Diagram- Coimbatore-Avinashi Road (AADD-2021)

Annexure-4A.

Coefficients of the predicted impact

	Code	Coefficients	Standard Error	t Stat	P-value	Lower 95.0%	Upper 95.0%
Constant	Y	0.6102	0.1808	3.3739	0.0012	0.2494	0.9710
Cd	X_1	1.7165	0.5999	2.8613	0.0056	0.5198	2.9133
Cr	X_2	-0.1058	0.0770	-1.3736	0.1740	-0.2594	0.0479
Cu	X_3	-0.2002	0.0658	-3.0449	0.0033	-0.3314	-0.0690
Fe	X_4	0.3101	0.0388	8.0003	0.0000	0.2327	0.3874
Pb	X_5	0.6214	0.2181	2.8495	0.0058	0.1864	1.0564
Zn	X_6	0.1066	0.0905	1.1780	0.2429	-0.0740	0.2872

The sum of the square is less than 0.45, the degree of freedom is shown table, its theoretical value is less than the experimental value, and the square of R indicates the non-linear equation from 76 observations, as shown in below table. It indicates that the model is significate to the predict the equation.

ANOVA & Regression Statistics of Outcome Summary

		ANOVA				Regression Statistics				
Sample Vol.	DF	SS	MS	F	Significance F	Multiple R	R^2	Adjusted R^2	Std. Error	Observations
Regression -6	51									
Residual-70	31	0.45	8.51	18.85	7.43E-13	0.79	0.62	0.59	0.67	76
Total -76	82									

D.D.: Degree Freedom, S.S.: Sum of square. MS: Mean Square F: Fisher factor

References

Acosta J.A., Faz A., Kalbitz K *et al.* (2014). Partitioning of heavy metals over different chemical fraction in street dust of Murcia (Spain) as a basis for risk assessment. *Journal of Geochemical Exploration,* **144**, 298–305. https://doi.org/ 10.1016/j.gexplo.2014.02.004.

Amato F., Cassee F.R., Denier van der Gon H.A.C *et al.* (2014). Urban air quality: The challenge of traffic non-exhaust emissions. *Journal of Hazardous Materials*, **275**, 31–36. https://doi.org/ 10.1016/j.jhazmat.2014.04.053.

Anerao P., Kaware R., Khedikar A.K *et al.* (2022). Phytoremediation of persistent organic pollutants: Concept challenges and perspectives. *Phytoremediation Technology for the Removal of Heavy Metals and Other Contaminants from Soil and Water* 375–404. https://doi.org/10.1016/B978-0-323-85763-5.00018-0.

Ayres R.U. (1997). Metals recycling: economic and environmental implications. *Resources, Conservation and Recycling* **21**, 145–173. https://doi.org/10.1016/S0921-3449(97)00033-5.

Bisht L., Gupta V., Singh A *et al.* (2022). Heavy metal concentration and its distribution analysis in urban road dust: A case study from most populated city of Indian state of Uttarakhand. *Spat Spatiotemporal Epidemiol*, **40**:. https://doi.org/10.1016/j.sste.2021.100470.

CCR (2021) CCR. In: Central Control Room for Air Quality Management - All India, Central Pollution Control Board, Ministry of Environment, Forest and Climate Change, Govt. of India. https://app.cpcbccr.com/ccr/#/caaqm-dashboard-all/caaqm-landing. Accessed 8 Dec 2021.

Chen X., Jiang W., Tong T *et al.* (2021). Molecular Interaction and Evolution of Jasmonate Signaling With Transport and Detoxification of Heavy Metals and Metalloids in Plants. Frontiers of Plant Science **12**,. https://doi.org/10.3389/FPLS.2021.665842/FULL.

Collazo-Ortega M., Rosas U. and Reyes-Santiago J. (2017). Towards Providing Solutions to the Air Quality Crisis in the Mexico City Metropolitan Area: Carbon Sequestration by Succulent Species in Green Roofs. PLoS Curr 9:. https://doi.org/10.1371/CURRENTS.DIS.BB66AE4F4F3C6EB118A019A29A9CE80F.

CSIR-CRRI. (2017). IHC Manual: CSIR-Central Road Research Institute.

Dhamaniya A. and Chandra S. (2016). Conceptual Approach for Estimating Dynamic Passenger Car Units on Urban Arterial Roads by Using Simultaneous Equations. Transportation Research Record. *Journal of the Transportation Research Board*, **2553**, 108–116. https://doi.org/10.3141/2553-12.

Guttikunda S.K., Goel R. and Pant P. (2014). Nature of air pollution, emission sources, and management in the Indian cities. Atmospheric Environment, **95**, 501–510. https://doi.org/10.1016/J.ATMOSENV.2014.07.006.

Hao X., Yi X., Dang Z. and Liang Y. (2022). Heavy Metal Sources, Contamination and Risk Assessment in Legacy Pb/Zn Mining Tailings Area: Field Soil and Simulated Rainfall. Bulletin of Environmental Contamination and Toxicology, 2022 109:4 109:636–642. https://doi.org/10.1007/S00128-022-03555-X.

Huang F., Liu B., Yu Y et al. (2022). Heavy metals in road dust across China: occurrence, sources and health risk assessment. Bulletin of Environmental Contamination and Toxicology, 109, 2, 109, 323–331. https://doi.org/10.1007/S00128-022-03558-8.

McNabola A., Broderick B.M. and Gill L.W. (2009). The impacts of inter-vehicle spacing on in-vehicle air pollution concentrations in idling urban traffic conditions. Transportation Research Part D: Transport and Environment, 14, 567–575. https://doi.org/10.1016/j.trd.2009.08.003.

MoRTH. (2018). Road Transport Year Book. In: Ministry of Road Transport & Highways, Government of India, Transport Research Wing, New Delhi. https://dorth.gov.in/road-transport-year-book-2017-18. Accessed 2 Jun, 2021.

MoRTH. (2019). Road transport year book. In: Ministry of Road Transport & Highways, Government of India, Transport Research Wing, New Delhi. https://dorth.gov.in/road-transport-year-book-2018-19. Accessed 2 Jul, 2021.

Nowak D.J., Hirabayashi S., Bodine A., Greenfield E. (2014). Tree and forest effects on air quality and human health in the United States. Environmental Pollution, 193, 119–129. https://doi.org/10.1016/j.envpol.2014.05.028.

Pouresmaieli M., Ataei M., Forouzandeh P et al. (2022). Recent progress on sustainable phytoremediation of heavy metals from soil. Journal of Environmental Chemical Engineering, 10, 108482. https://doi.org/10.1016/J.JECE.2022.108482.

Road and Transport (2020) Statistical Hand Book, 2020. In: Open Government Data Portal Tamil Nadu. https://tn.data.gov.in/catalog/statistical-hand-book-2020-road-and-transport#web_catalog_tabs_block_10. Accessed 8 Feb, 2021.

Saeedi M., Hosseinzadeh M., Jamshidi A. and Pajooheshfar SP (2009) Assessment of heavy metals contamination and leaching characteristics in highway side soils, Iran. Environ Monit Assess 151:231–241. https://doi.org/10.1007/s10661-008-0264-z.

Sharma M. and Biswas S (2021) Estimation of Passenger Car Unit on urban roads: A literature review. International Journal of Transportation Science and Technology 10:283–298

Solcast (2021) Solar Forecasting & Solar Irradiance Data. In: Solcast, 2019. Global solar irradiance data and PV system poweroutput data. https://www.solcast.com/. Accessed 1 Jul, 2021.

Su TH, Lin CS, Lu SY, et al (2022) Effect of air quality improvement by urban parks on mitigating PM2.5 and its associated heavy metals: A mobile-monitoring field study. Journal of Environmental Management, 323, 116283. https://doi.org/10.1016/J.JENVMAN.2022.116283.

Tiwari A., Kumar P. and Baldauf R., et al (2019) Considerations for evaluating green infrastructure impacts in microscale and macroscale air pollution dispersion models. Science of the Total Environment 672:410–426. https://doi.org/10.1016/j.scitotenv.2019.03.350.

Vats I., Singhal D., Tripathy S. and Jena SK (2022) The transition from BS4 to BS6 compliant vehicles for eco-friendly mobility in India: An empirical study on switching intention. Research in Transportation Economics 91:101131. https://doi.org/10.1016/J.RETREC.2021.101131.